

Unlocking Color and Flavor in Superconducting Strange Quark Matter

Mark Alford, Jürgen Berges, Krishna Rajagopal

Center for Theoretical Physics,
Massachusetts Institute of Technology, Cambridge, MA 02139

MIT-CTP-2844

Abstract

We explore the phase diagram of strongly interacting matter with massless u and d quarks as a function of the strange quark mass m_s and the chemical potential μ for baryon number. Neglecting electromagnetism, we describe the different baryonic and quark matter phases at zero temperature. For quark matter, we support our model-independent arguments with a quantitative analysis of a model which uses a four-fermion interaction abstracted from single-gluon exchange. For any finite m_s , at sufficiently large μ we find quark matter in a color-flavor locked state which leaves a global vector-like $SU(2)_{\text{color}+L+R}$ symmetry unbroken. As a consequence, chiral symmetry is always broken in sufficiently dense quark matter. As the density is reduced, for sufficiently large m_s we observe a first order transition from the color-flavor locked phase to a color superconducting phase analogous to that in two flavor QCD. At this unlocking transition chiral symmetry is restored. For realistic values of m_s our analysis indicates that chiral symmetry breaking may be present for all densities down to those characteristic of baryonic matter. This supports the idea that quark matter and baryonic matter may be continuously connected in nature. We map the gaps at the quark Fermi surfaces in the high density color-flavor locked phase onto gaps at the baryon Fermi surfaces at low densities.

1 Introduction and Phase Diagram

Strongly interacting matter at high baryon number density and low temperature is far less well understood than strongly interacting matter at high temperature and zero baryon number density. At high temperatures, the symmetry of the lowest free energy state is not in dispute, calculations using lattice gauge theory are bringing the equilibrium thermodynamics under reasonable quantitative control, and even non-equilibrium dynamical questions are being addressed. At high densities, we are still learning about the symmetries of the lowest free energy state. In addition to being of fundamental interest, an understanding of the symmetry properties of dense matter can be expected to inform our understanding of neutron star astrophysics and perhaps also heavy ion collisions which achieve high baryon densities without reaching very high temperatures.

At high densities and low temperatures, the relevant degrees of freedom are those which involve quarks with momenta near the Fermi surface(s). The presence of an arbitrarily weak attraction between pairs of quarks results in the formation of a condensate of quark Cooper pairs. Pairs of quarks cannot be color singlets, and in QCD with two flavors of massless quarks the Cooper pairs form in the color $\bar{\mathbf{3}}$ channel.[1, 2, 3, 4, 5] The resulting condensate gives gaps to quarks with two of three colors and breaks the local color symmetry $SU(3)_{\text{color}}$ to an $SU(2)_{\text{color}}$ subgroup. The breaking of a gauge symmetry cannot be characterized by a gauge invariant local order parameter which vanishes on one side of a phase boundary. The superconducting phase can be characterized rigorously only by its global symmetries. In QCD with two flavors, the Cooper pairs are $ud - du$ flavor singlets and, in particular, the global flavor $SU(2)_L \times SU(2)_R$ symmetry is left intact. There is an unbroken global symmetry which plays the role of baryon number symmetry, $U(1)_B$. Thus, no global symmetries are broken and the only putative Goldstone bosons are those five which become the longitudinal parts of the five gluons which acquire masses.[3]¹

In QCD with three flavors of massless quarks the Cooper pairs *cannot* be flavor singlets, and both color and flavor symmetries are necessarily broken. The symmetries of the phase which results have been analyzed in Ref. [6]. The attractive channel favored by one-gluon exchange exhibits “color-flavor locking”. It locks $SU(3)_L$ flavor rotations to $SU(3)_{\text{color}}$, in the sense that the condensate is not symmetric under either alone, but is symmetric under the simultaneous $SU(3)_{\text{color}+L}$ rotations. The condensate also locks $SU(3)_R$ rotations to $SU(3)_{\text{color}}$, and since color is a vector symmetry the chiral $SU(3)_{L-R}$ symmetry is broken. Thus, in quark matter with three massless quarks, the $SU(3)_{\text{color}} \times SU(3)_L \times$

¹There is also an unbroken gauged symmetry which plays the role of electromagnetism. Also, the third color quarks can condense,[3] as we discuss below, but the resulting gap is much smaller.

$SU(3)_R \times U(1)_B$ symmetry is broken down to the global diagonal $SU(3)_{\text{color}+V}$ subgroup. There is also an unbroken gauged $U(1)$ symmetry (under which all quarks have integer charges) which plays the role of electromagnetism. All nine quarks have a gap. All eight gluons get a mass. There are nine massless Nambu Goldstone excitations of the condensate of Cooper pairs which result from the breaking of the axial $SU(3)_A$ and baryon number $U(1)_B$. We see that cold dense quark matter has rather different global symmetries for $m_s = 0$ than for $m_s = \infty$.

A nonzero strange quark mass explicitly breaks the flavor $SU(3)_V$ symmetry. As a consequence, color-flavor locking with an unbroken global $SU(3)_{\text{color}+V}$ occurs only for $m_s \equiv 0$. Instead, for nonzero but sufficiently small strange quark mass we expect, and find, color-flavor locking which leaves a global $SU(2)_{\text{color}+V}$ group unbroken. As m_s is increased from zero to infinity, there has to be some value m_s^{unlock} at which color and flavor rotations are unlocked, and the full $SU(2)_L \times SU(2)_R$ symmetry is restored. We argue on general grounds in Section 2 that this unlocking phase transition must be of first order. In subsequent Sections, we analyze this transition quantitatively in a model using a four-fermion interaction with quantum numbers abstracted from single-gluon exchange.

From our analysis of the unlocking transition, we conclude that for realistic values of the strange quark mass chiral symmetry breaking may be present for densities all the way down to those characteristic of baryonic matter. This raises the possibility that quark matter and baryonic matter may be continuously connected in nature, as Schäfer and Wilczek have conjectured for QCD with three massless quarks.[7] We use our calculations of the properties of color-flavor locked superconducting strange quark matter to map the gaps due to pairing at the quark Fermi surfaces onto gaps due to pairing at the baryon Fermi surfaces in superfluid baryonic matter consisting of nucleons, Λ 's, Σ 's, and Ξ 's. (See Section 6).

We argue that color-flavor locking will always occur for sufficiently large chemical potential, for any nonzero, finite m_s . We make this argument by first using our results as a guide to quark matter at moderate densities and then using them to normalize Son's model-independent analysis valid at very high densities.[8] As a consequence of color-flavor locking, chiral symmetry is spontaneously broken even at asymptotically high densities, in sharp contrast to the well established restoration of chiral symmetry at high temperature.

Our goal in this paper is a consistent picture of the symmetries of cold dense quark matter with massless u and d quarks as a function of the strange quark mass m_s and the chemical potential μ . We take μ to be the chemical potential for quark number, one third that for baryon number. m_s is the current quark mass; we will refer to the μ -dependent constituent quark mass as $M_s(\mu)$.

Figure 1 summarizes our conjecture for the zero temperature phase diagram of QCD as a function of m_s and μ . (We work at zero temperature throughout this

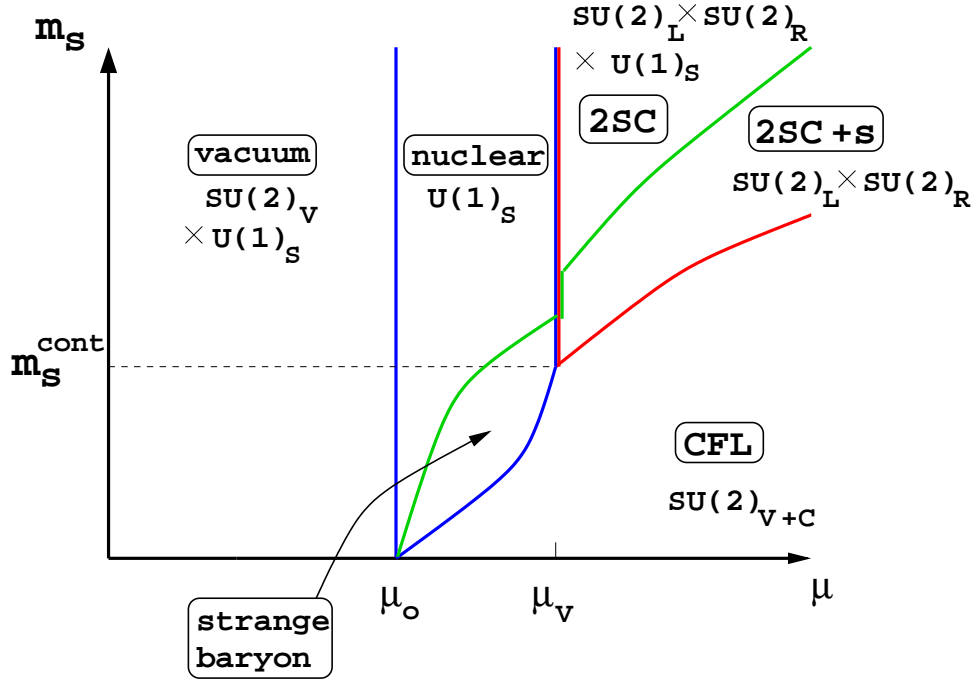


Figure 1: Conjectured phase diagram for QCD with two massless quarks and a strange quark at zero temperature. The global symmetries of each phase are labelled. The regions of the phase diagram labelled 2SC, 2SC+s and CFL denote color superconducting quark matter phases. The Figure is described at length in the text.

paper.) The rest of this section can be read as a description of this Figure. Lines in the diagram separate phases which differ in their global symmetries. This means that each line describes a distinction which can be associated with a local order parameter which vanishes on one side of the line. In each region of the diagram, we list the unbroken global symmetries of the corresponding phase. We characterize the phases using the $SU(2)_L \times SU(2)_R$ flavor rotations of the light quarks, and the $U(1)_S$ rotations of the strange quarks.²

In subsequent Sections of this paper, we explore those phases (labelled 2SC, 2SC+s and CFL) which extend to high enough density that they can be described as superconducting quark matter. We analyze these phases, and the unlocking phase transition which separates them, quantitatively in a model in which quarks

²The $U(1)_B$ symmetry associated with baryon number is a combination of $U(1)_S$, a $U(1)$ subgroup of isospin, and the gauged $U(1)_{EM}$ of electromagnetism. Therefore, in our analysis of the global symmetries, once we have analyzed isospin and strangeness, considering baryon number adds nothing new.

interact via a four-quark interaction modelled on that induced by single-gluon exchange. Certainly, our model is not expected to be a valid description for QCD at nuclear matter density, where confinement plays an important role. That part of the diagram which describes the symmetry properties of different phases of baryonic matter is therefore not derived from our model. It is conjectural but plausible.

In Figure 1 and throughout this paper, we neglect the small u and d current quark masses. The light quark masses have no substantial influence on the condensation of quark Cooper pairs.[5, 9] We also ignore the effects of electromagnetism throughout. We assume that wherever a baryon Fermi surface is present, baryons always pair at zero temperature. To simplify our analysis, we assume that baryons always pair in channels which preserve rotational invariance, breaking internal symmetries such as isospin if necessary.

We now explain the features shown in Figure 1 by beginning at $\mu = 0$ (in vacuum) and describing the phase transitions which occur as μ is increased at constant m_s . We do this twice, first with a large enough value of m_s that the strange quark is heavy enough that immediately above deconfinement μ is still less than m_s and there are still no strange quarks present. For $\mu = 0$ the density is zero; isospin and strangeness are unbroken; Lorentz symmetry is unbroken; chiral symmetry is broken. Above a first order transition³ at an onset chemical potential $\mu_o \sim 300$ MeV, one finds nuclear matter (“nuclear” in Figure 1). Lorentz symmetry is broken, leaving only rotational symmetry manifest. Chiral symmetry is thought to be broken, although the chiral condensate $\langle \bar{q}q \rangle$ is expected to be reduced from its vacuum value. In the nuclear matter phase, we expect an instability of the nucleon Fermi surfaces to lead to Cooper pairing. We assume that (as is observed in nuclei) the pairing is pp and nn , breaking isospin. Since there are no strange baryons present, $U(1)_S$ is unbroken.

At the large value of m_s we are currently describing, when μ is increased above μ_V , we find the “2SC” phase of color-superconducting matter consisting of up and down quarks only, described in Refs. [1, 2, 3, 4]. A nucleon description is no longer appropriate. The light quarks pair in isosinglet channels. $SU(2)_V$ is unbroken. $SU(2)_A$ is unbroken. Quarks of two colors pair in a Lorentz singlet channel; quarks carrying the third color can form an axial vector (ferromagnetic) condensate, which breaks rotational invariance. The associated gap is of order a keV or much less[3] and we neglect this condensate in Figure 1.⁴ The phase transition at μ_V is first

³Discussed in Ref. [10].

⁴In a mean-field treatment, one gluon exchange is neither attractive nor repulsive in the channel which leads to the ferromagnetic condensate while the instanton interaction is only weakly attractive. The ferromagnetic condensate is therefore fragile in the sense that this channel could easily be rendered repulsive by other interactions.[3] If that were the case, the third color quarks would presumably form Cooper pairs with nonzero orbital angular momentum, and an

order [3, 4, 5, 11, 9, 12] and is characterized by a competition between the chiral $\langle \bar{q}q \rangle$ condensate and the superconducting $\langle qq \rangle$ condensate.[5, 12]

As the chemical potential is increased further, when μ exceeds the constituent strange quark mass $M_s(\mu)$ a strange quark Fermi surface forms, with a Fermi momentum far below that for the light quarks. We denote the resulting phase “2SC+s”. Light and strange quarks do not pair with each other, because their respective Fermi momenta are so different (see Section 2). The strange Fermi surface is presumably nevertheless unstable. The resulting ss condensate must be constructed from Cooper pairs which are either color **6**, or have spin 1, or have nonzero angular momentum, or must be $\langle sC\gamma_4s \rangle$, which is symmetric in Dirac indices. Each of these options lead to small gaps, for different reasons: One-gluon exchange is repulsive in rotationally invariant color **6** channels and the $\langle sC\gamma_4s \rangle$ channel, and although other interactions may overcome this and result in a net attraction, this is likely to be much weaker than the attraction in the dominant color **$\bar{3}$** channels. Gaps involving Cooper pairs with nonzero J tend to be significantly suppressed because not all quarks at the Fermi surface participate.[3] Thus, although $U(1)_S$ will be broken in the “2SC+s” phase by an ss condensate in *some* channel, we expect that the resulting gaps will be very small. In our analysis below we therefore neglect the difference between the 2SC and 2SC+s phases.

Finally, when the chemical potential is high enough that the Fermi momenta for the strange and light quarks become comparable, we cross the first order locking transition described in detail in the next Sections, and find the color-flavor locked (CFL) phase. There is an unbroken global symmetry constructed by locking the $SU(2)_V$ isospin rotations and an $SU(2)$ subgroup of color. Chiral symmetry is once again broken.

We now describe the sequence of phases which arise as μ is increased, this time for a value of m_s small enough that strange baryonic matter forms below the deconfinement density. At μ_c , one enters the nuclear matter phase, with the familiar nn and pp pairing at the neutron and proton Fermi surfaces breaking isospin. The Λ , Σ and Ξ densities are still zero, and strangeness is unbroken. At a somewhat larger chemical potential, we enter the strange baryonic matter phase, with Fermi surfaces for the Λ and Σ . These pair with themselves in spin singlets, breaking $U(1)_S$. This phase is labelled “strange baryon” in Figure 1. The global symmetries $SU(2)_L \times SU(2)_R$ and $U(1)_S$ are all broken. As μ rises, one finds yet another onset at which the Ξ density becomes nonzero. This breaks no new symmetries, and so is not shown in the Figure. Note that kaon condensation[13] breaks $U(1)_S$, and $SU(2)_V$. The only phase in the diagram in which this occurs is that which we have labelled the strange baryon phase. Thus, if kaon condensation occurs, by definition it occurs within this region of the diagram.

even smaller gap.

If kaon condensation is favored, this will tend to enlarge the region of the diagram within which $U(1)_S$ and $SU(2)_V$ are both broken.

We can imagine two possibilities for what happens next as μ increases further. (1) Deconfinement: the baryonic Fermi surface is replaced by u, d, s quark Fermi surfaces, which are unstable against pairing, and we enter the CFL phase, described above. Isospin is locked to color and $SU(2)_{\text{color}+V}$ is restored, but chiral symmetry remains broken. (2) No deconfinement: the Fermi momenta of all of the octet baryons are now similar enough that pairing between baryons with differing strangeness becomes possible. At this point, isospin is restored: the baryons pair in rotationally invariant isosinglets ($p\Xi^-$, $n\Xi^0$, $\Sigma^+\Sigma^-$, $\Sigma^0\Sigma^0$, $\Lambda\Lambda$). The interesting point is that scenario (1) and scenario (2) are indistinguishable. Both look like the “CFL” phase of the figure: $U(1)_S$ and chirality are broken, and there is an unbroken vector $SU(2)$. This is the “continuity of quark and hadron matter” described by Schäfer and Wilczek [7]. We conclude that for low enough strange quark mass, $m_s < m_s^{\text{cont}}$, there may be a region where sufficiently dense baryonic matter has the same symmetries as quark matter, and there need not be any phase transition between them. In Section 6 we use this observation to construct a mapping between the gaps we have calculated at the Fermi surfaces in the quark matter phase and gaps at the baryonic Fermi surfaces at lower densities.

All of the qualitative features shown in Figure 1 follow from the above discussion of the small and large m_s regimes, with one exception. In Figure 1, a transition between two flavor nuclear matter and three flavor quark matter (in the 2SC+s phase) occurs only for a range of values of m_s above m_s^{cont} . However, it may be that the strange baryon phase ends *below* m_s^{cont} . One would then have a transition between two flavor nuclear matter and three flavor quark matter (in either the 2SC+s phase or the CFL phase) for a range of m_s values which extends both above and below m_s^{cont} . Determining the extent of the strange baryon phase requires a detailed analysis of strange baryonic matter, including the possibility of kaon condensation. This is not our goal here.

This concludes our overview of the qualitative features of the phase diagram for low temperature strongly interacting matter. In subsequent sections we analyze the 2SC and CFL phases and the unlocking transition more quantitatively, and use the properties of the CFL phase to make predictions for properties of baryonic matter in which $U(1)_S$ is broken while $SU(2)_V$ is unbroken.

2 Model Independent Features of the Unlocking Phase Transition

In this section, we give a model independent argument that the unlocking phase transition between the CFL and 2SC phases in Figure 1 must be first order.

For any $m_s \neq 0$, transformations in $SU(3)_A$ which involve the strange quark are explicitly not symmetries. The CFL and 2SC phases are distinguished by whether the chiral $SU(2)_A$ rotations involving only the u and d quarks are or are not spontaneously broken. As we will make clear in subsequent sections, the unlocking transition is associated with the vanishing of those diquark condensates which pair a strange quark with either an up or a down quark. We denote the resulting gaps Δ_{us} for simplicity. In the absence of any Δ_{us} gap, the only Cooper pairs are those involving pairs of light quarks, or pairs of strange quarks. The light quark condensate is unaffected by the strange quarks, and behaves as in a theory with only two flavors of quarks. Chiral symmetry is unbroken. We will show explicitly below that when $\Delta_{us} \neq 0$, the interaction between the light quark condensates and the mixed (light and strange) condensate results in the breaking of two-flavor chiral symmetry $SU(2)_A$ via the locking of $SU(2)_L$ and $SU(2)_R$ flavor symmetries to an $SU(2)$ subgroup of color. This color-flavor locking mechanism leaves a global $SU(2)_{\text{color}+V}$ group unbroken.

The unlocking transition is a transition between a phase with $\Delta_{us} \neq 0$ at $M_s < M_s^{\text{unlock}}$ and a phase with $\Delta_{us} = 0$. ($M_s(\mu)$ is the constituent strange quark mass at chemical potential μ .) The BCS mechanism guarantees superconductivity in the presence of an arbitrarily weak attractive interaction, and there is certainly an attraction between u and s quarks (with color $\bar{\mathbf{3}}$) for any M_s . How, then, can Δ_{us} vanish above M_s^{unlock} ? The BCS result relies on a singularity which arises for pairs of fermions with zero total momentum *at* the Fermi surface. We see from Figure 2 that no pairing is possible for quarks with momenta between the u and s Fermi momenta, and that at most one of the quarks in a u - s Cooper pair can be at its respective Fermi surface. The BCS singularity therefore does not arise if $M_s \neq 0$, and a u - s condensate is not mandatory. A u - s condensate involves pairing of quarks with momenta within about Δ_{us} of the Fermi surface, and we therefore expect that Δ_{us} can only be nonzero if the mismatch between the up and strange Fermi momenta is less than or of order Δ_{us} :

$$\sqrt{\mu^2 - M_u(\mu)^2} - \sqrt{\mu^2 - M_s(\mu)^2} \approx \frac{M_s(\mu)^2 - M_u(\mu)^2}{2\mu} \lesssim \Delta_{us} . \quad (2.1)$$

Here $M_s(\mu)$ and $M_u(\mu)$ are the constituent quark masses in the CFL phase. We neglect $M_u(\mu)$ in the following. Equation (2.1) implies that arbitrarily small values of Δ_{us} are impossible. As m_s is increased from zero, Δ_{us} decreases until it is comparable to $M_s(\mu)^2/2\mu$. At this point, smaller nonzero values of Δ_{us} are not possible, and Δ_{us} must therefore vanish discontinuously. This simple physical argument leads us to conclude that the unlocking phase transition at $M_s = M_s^{\text{unlock}}$ must be first order.

Below, we confirm by explicit calculation in a model that the unlocking phase transition is first order. We find that Δ_{us} is of order 50 – 100 MeV on the CFL

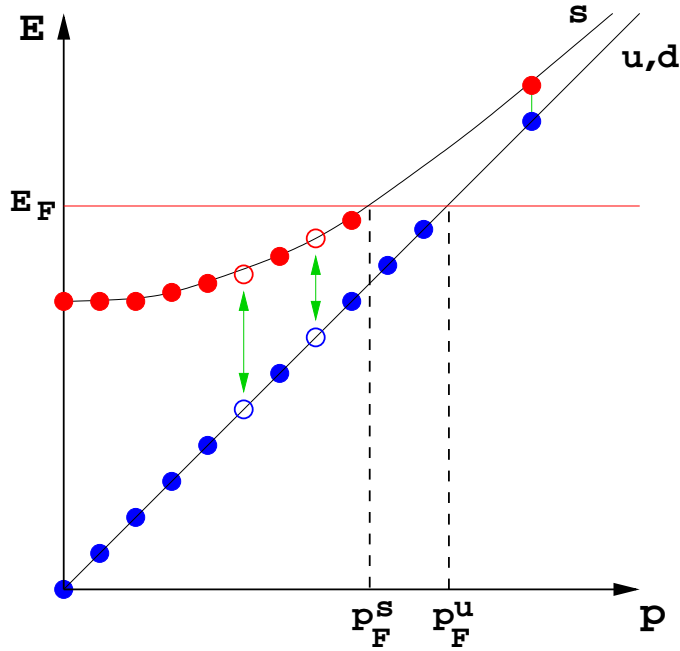


Figure 2: How the strange quark mass disrupts a u - s condensate. The strange quark (upper curve) and light quark (straight line) dispersion relations are shown, with their Fermi seas filled up to the Fermi energy E_F . The horizontal axis is the magnitude of the spatial momentum; pairing occurs between particles (or holes) with the same p and opposite \vec{p} . For $p < p_F^s$, hole-hole pairing ($\bar{s}\bar{u}$) is possible (two examples are shown). For $p > p_F^u$, particle-particle pairing (s - u) is possible (one example is shown). Between the Fermi momenta for the s and u quarks, no such pairing is possible.

side of the transition if the coupling is calibrated to give a reasonable magnitude for the chiral condensate in vacuum.

3 Superconducting Condensates in a Model

We study the physics of the quark matter phases in Figure 1 in a toy model in which we replace the full interactions between quarks by a four-fermion interaction with the quantum numbers of single-gluon exchange,

$$\mathcal{L}_{\text{interaction}} = G \int d^4x (\bar{q}\lambda^A\gamma^\mu q) (\bar{q}\lambda^A\gamma_\mu q) , \quad (3.1)$$

and work in a mean-field approximation. All four-fermion interactions involving fermions at the Fermi surface are equally relevant, in the renormalization group

sense, so why use only the one with the quantum numbers of one-gluon exchange? Renormalization group analyses[14, 15] show that other interactions are important, but confirm that in QCD with two and three massless quarks the most attractive channels for condensation are those generated by (3.1). There is one important caveat. The single-gluon-exchange interaction is symmetric under $U(1)_A$, and so it sees no distinction between condensates of the form $\langle qCq \rangle$ and $\langle qC\gamma_5q \rangle$. However, once instantons are included the Lorentz scalar $\langle qC\gamma_5q \rangle$ is favored,[3, 4] so we neglect the other form.

One of the central qualitative lessons of past work is that superconducting gaps of order 100 MeV are obtained in the quark matter phase independent of the details of the interaction which is used, as long as the strength of the interaction is chosen in a way which is roughly consistent with what we know about the vacuum chiral condensate. Superconducting gaps of this magnitude can be obtained using a number of different treatments based upon single-gluon exchange.[2, 16, 6] Refs. [3, 4, 5, 12] find gaps of this magnitude by making approximations of varying sophistication in which the interaction between quarks is modeled by that induced by instantons. Further confirmation of this lesson comes from recent work using the NJL model.[17]

As in any model which uses a four-fermion interaction, in addition to choosing the quantum numbers of the interaction we must introduce an ad hoc form factor. The explicit lesson of Refs. [3, 6, 17], implicit in other work, is that results are rather insensitive to the choice of form factor, again as long as G is suitably normalized. We therefore use a simple sharp cutoff in momentum integrals at a spatial momentum $\Lambda = 800$ MeV. Our results should therefore not be extended above $\mu \sim \Lambda$. The form factor (which we describe by the single parameter Λ) is a crude representation of physics not described by the model, and Λ should not be taken to infinity. For $\Lambda = 0.8$ GeV, setting $G = 7.5$ GeV⁻² in (3.1) results in a vacuum constituent mass for the light quarks of 400 MeV, and we use these values of Λ and G throughout. We have however checked that if we instead take $\Lambda = 1$ GeV, and change G accordingly, the superconducting gaps and the location of the unlocking phase transition are not significantly affected.

An analysis of the phase diagram requires condensates

$$\langle q_i^\alpha C\gamma_5 q_j^\beta \rangle, \quad \langle q_i^\alpha C\gamma_5\gamma_4 q_j^\beta \rangle, \quad \langle \bar{q}_\alpha^i q_j^\beta \rangle, \quad (3.2)$$

leading to gap parameters

$$\Delta_{ij}^{\alpha\beta}, \quad \kappa_{ij}^{\alpha\beta}, \quad \phi_{\alpha j}^{i\beta} \quad (3.3)$$

with corresponding quantum numbers. Each gap matrix is a symmetric 9×9 matrix describing the color (Greek indices) and flavor (Roman indices) structure.

In Appendix A we derive the gap equation for these condensates in full generality, assuming nothing about their color-flavor structure. However, it is very difficult to solve the general gap equation, so at this point we make several simplifying assumptions to obtain easily soluble gap equations. These are:

1. We fix $\phi_{\alpha j}^{i\beta} = M_s \delta_3^i \delta_j^3 \delta_\alpha^\beta$. For more details see below.
2. We use the simplest form for $\Delta_{ij}^{\alpha\beta}$ which allows an interpolation between the color-flavor locking favored by single-gluon exchange at $m_s = 0$ and the “2SC” phase favored at $m_s \rightarrow \infty$ (see (3.4)). This ansatz, which requires five independent superconducting gap parameters, leads to consistent gap equations in the presence of the one-gluon exchange interaction. We describe this ansatz in detail in Section 4.
3. We neglect $\kappa_{ij}^{\alpha\beta}$. This condensate pairs left-handed and right-handed quarks, and so breaks chiral symmetry. It can be shown to vanish in the absence of quark masses.[18] In Appendix A we show that it *must* be nonzero in the presence of a nonzero $\langle qC\gamma_5 q \rangle$ condensate and nonzero quark masses. In the 2SC phase, the $\langle qC\gamma_5 q \rangle$ condensate involves only the massless quarks and $\langle qC\gamma_5\gamma_4 q \rangle$ therefore vanishes and chiral symmetry remains unbroken. In the CFL phase, however, the $\langle qC\gamma_5 q \rangle$ condensate involves the massive strange quarks and itself breaks chiral symmetry by color-flavor locking. No symmetry argument precludes $\kappa \neq 0$, and in Appendix A we have confirmed by direct calculation at one value of μ that the gaps $\kappa_{ij}^{\alpha\beta}$ are nonzero in the CFL phase. However, we find that these gaps are much smaller than the corresponding gaps generated by the $\langle qC\gamma_5 q \rangle$ condensate. Including κ in the gap equations for Δ makes finding solutions prohibitively slow. Therefore, once we have convinced ourselves that these condensates are present but small, we neglect them.

We now give a more detailed discussion of our assumptions about the quark mass matrix ϕ . Since all our calculations are in the quark matter regime ($\mu > \mu_V$ in Figure 1), we will assume that μ is high enough that we can neglect chiral condensates for the u and d quarks,⁵ but because the current quark mass m_s is nonzero there may be a nonzero $\langle \bar{s}s \rangle$ chiral condensate. In this case the quark mass matrix is $\phi = \text{diag}(0, 0, M_s)$, where M_s is the μ -dependent constituent strange quark mass, satisfying a gap equation of its own. At sufficiently high densities, it

⁵ Because chiral symmetry is broken in the CFL phase, there is no reason for the ordinary $\langle \bar{u}u \rangle$ and $\langle \bar{d}d \rangle$ chiral condensate to vanish. Indeed, Ref. [6] demonstrates that the $\langle \bar{u}u \rangle$ and $\langle \bar{d}d \rangle$ condensates must be nonvanishing. However, an explicit calculation [19] shows them to be small, and we neglect them. Eq. (2.1) shows that nonzero $\langle \bar{u}u \rangle$ and $\langle \bar{d}d \rangle$ condensates allow color-flavor locking to persist to higher strange quark masses.

is given by the current mass m_s , of order 100 MeV. At lower densities, it receives an additional contribution from $\langle \bar{s}s \rangle$. In the interests of simplicity, however, we will not solve the M_s gap equation simultaneously with the superconductivity gap equations. Instead, we treat M_s as a parameter in the superconductivity gap equations, and do not determine what value of M_s corresponds to given values of m_s and μ . For simplicity, we choose the same value of the parameter M_s for strange quarks of all three colors. This would not be the case in a treatment in which the M_s gap equations are solved simultaneously with the superconductivity gap equations.[12]

With our simplifying assumptions, we are left needing only a gap equation for the quark-quark condensate $\Delta_{ij}^{\alpha\beta}$. The simplest ansatz that interpolates between the two flavor case ($m_s = \infty$) and the three flavor case ($m_s = 0$) is

$$\Delta_{ij}^{\alpha\beta} = \begin{pmatrix} b+e & b & c & & & & & & \\ & b & b+e & c & & & & & \\ & c & c & d & & & & & \\ & & & & e & & & & \\ & & & e & & & & & \\ & & & & & f & & & \\ & & & & & f & & & \\ & & & & & & f & & \\ & & & & & & & f & \\ & & & & & & & & f \end{pmatrix} \quad (3.4)$$

basis vectors:

$$\begin{aligned} (\alpha, i) &= (1, 1), (2, 2), (3, 3), (1, 2), (2, 1), (1, 3), (3, 1), (2, 3), (3, 2) \\ &= (r, u), (g, d), (b, s), (r, d), (g, u), (r, s), (b, u), (g, s), (b, d) \end{aligned}$$

where the color indices are α, β and the flavor indices are i, j . The strange quark is $i = 3$. The rows are labelled by (α, i) and the columns by (β, j) .

description	condensate	symmetry
2SC: 2-flavor superconductivity	$c = d = f = 0,$ $b = -e$	$SU(2)_L \times SU(2)_R$
CFL: color-flavor locking		$SU(2)_{\text{color}+L+R}$
CFL: color-flavor locking with $m_s = 0$	$c = b, f = e,$ $d = b + e$	$SU(3)_{\text{color}+L+R}$

Table 1: Symmetries of the condensate ansatz (3.4) in various regimes.

The properties of the ansatz are summarized in Table 1. In its general form, this condensate locks color and flavor. This is because of the condensates c and

f , referred to collectively as Δ_{us} above, that combine a strange quark with a light one. It is straightforward to confirm by direct calculation that if either c or f or $b+e$ is nonzero, then the matrix $\Delta_{ij}^{\alpha\beta}$ of (3.4) is not invariant under separate flavor or color rotations but is left invariant by simultaneous rotations of $SU(2)_V$ and the $SU(2)$ subgroup of color corresponding to the colors 1 and 2. Thus, color-flavor locking occurs whenever one or more of c , f , or $b+e$ is nonzero. We discuss $b+e$ below.

Although the standard electromagnetic symmetry is broken in the CFL phase, as are all the color gauge symmetries, there is a combination of electromagnetic and color symmetry that is preserved.[6] Consider the gauged $U(1)$ under which the charge Q' of each quark is the sum of its electromagnetic charge ($2/3, -1/3, -1/3$) (depending on the flavor of the quark) and its color hypercharge ($-2/3, 1/3, 1/3$) (depending on the color of the quark). It is easy to confirm that the sum of the Q' charges of each pair of quarks corresponding to a nonzero entry in (3.4) is zero. This modified electromagnetism is therefore not broken by the condensate.

At $M_s = 0$, one has color-flavor locking: c , f and $b+e$ are all nonzero. In addition, $c = b$, $f = e$, and $d = b+e$, and the matrix is invariant under simultaneous rotations of $SU(3)_V$ and $SU(3)_{\text{color}}$. For M_s nonzero but sufficiently small, c , f and $b+e$ remain nonzero but are no longer equal to b , e and d . Color and flavor are locked, and the matrix is invariant under simultaneous rotations of $SU(2)_V$ and $SU(2)_{\text{color}}$. As described in Section 2, once M_s becomes large enough, c and f both vanish (and so does $b+e$) and the symmetry group enlarges, unlocking color and flavor, and restoring chiral symmetry (see Table 1).

If Δ were nonzero only in color $\bar{\mathbf{3}}$ channels, we would have $b = -e$, $d = 0$ and $c = -f$. Single-gluon-exchange is repulsive in the color $\mathbf{6}$ channels. However, in the CFL phase where c and f are nonzero, the only consistent solutions to the gap equations have $b \neq -e$, $c \neq -f$, and $d \neq 0$. This means that the single-gluon-exchange interaction *requires* a small color $\mathbf{6}$ admixture along with the favored color $\bar{\mathbf{3}}$ condensate, even though it prohibits color $\mathbf{6}$ condensates alone. This feature occurs both for $M_s = 0$ [6] and for $0 < M_s < M_s^{\text{unlock}}$. Note that not all color $\mathbf{6}$ terms arise in (3.4). For example, only three of the nine diagonal elements of (3.4) are nonzero. These are the only three diagonal elements which can be nonzero without breaking the $SU(2)_{\text{color}+V}$ symmetry, and upsetting color-flavor locking. Furthermore, if the two upper-most diagonal elements were not equal to $b+e$, the $SU(2)_{\text{color}+V}$ symmetry would also be broken. We have therefore learned that the color $\mathbf{6}$ terms which are induced in the presence of a color $\bar{\mathbf{3}}$ condensate are those which do not change the global symmetry of the color $\bar{\mathbf{3}}$ condensate. Those color $\mathbf{6}$ terms which are “allowed” in this sense are generated by the interaction.

The corresponding analysis of the 2SC phase, where only two flavors participate in the condensate is similar in logic but leads to different conclusions. In the 2SC

phase, where c and f are zero, we do in fact find $b = -e$ and $d = 0$, namely a pure color $\bar{\mathbf{3}}$ condensate. In this case, if $b + e$ were nonzero, one *would* have color-flavor locking and broken chiral symmetry. In this case, then, the pure color $\bar{\mathbf{3}}$ condensate with $b + e = 0$ is “protected” by the fact that any admixture of color $\mathbf{6}$ condensate like $b + e$ would break a global symmetry which the color $\bar{\mathbf{3}}$ condensate does not break. In the absence of c and f , a nonzero d condensate ($\langle ss \rangle$) is still allowed, but there is no way for the color $\bar{\mathbf{3}}$ condensate to induce it. Therefore the simple argument that one-gluon exchange is repulsive in this channel holds, and in our model we find $d = 0$ in the 2SC phase even where the strange quark density is nonzero. As discussed above, a more complete analysis would include a small $\langle ss \rangle$ condensate in some channel, resulting in a distinction between the 2SC and 2SC+s phases which our analysis does not see.

4 The Gap Equation ...

Our task now is to obtain the gap equation for Δ , and verify the behavior described in Sections 1 and 2. In particular, we want to show that the unlocking phase transition is first-order, and calculate $M_s^{\text{unlock}}(\mu)$ and compare to the criterion (2.1) which we derived on model-independent grounds.

In Appendix A we have derived the mean field gap equation and given its general solution. It takes the form (see Eq. (A.5))

$$\Delta = \frac{G}{(2\pi)^4} \int d^4q \lambda_A^T \gamma_\mu P_1(\mu, M_s, \Delta, q) \lambda_A \gamma^\mu, \quad (4.1)$$

where the function P_1 is given by (A.6) and (A.7), and we are assuming, as described in Section 3 that $\phi_{\alpha j}^{i\beta} = M_s \delta_3^i \delta_j^3 \delta_\alpha^\beta$ and that $\kappa = 0$. Note that strictly speaking the gap equations do not close for $\kappa = 0$. The κ gap equation is just like (4.1) but with $-P_4$ instead of P_1 on the right hand side, and for $M_s > 0$, P_4 is nonzero even when $\kappa = 0$. This means that it is inconsistent to set $\kappa = 0$. However, as discussed in the Appendix, κ turns out to be small and we use (4.1) with $\kappa = 0$ in P_1 .

In principle we could just evaluate $P_1(\mu, M_s, \Delta, q)$ by substituting (3.4) into (A.7), but that would lead to a very complicated expression. To turn (4.1) into a tractable set of gap equations, we transform to a slightly different basis from (3.4). In the new basis, the first 2 vectors are $(\alpha, i) = 1/\sqrt{2}((1, 1) \pm (2, 2))$. Now the top left 3×3 block of (3.4) looks like

$$\begin{pmatrix} e & & \\ & a_{11} & a_{12} \\ & a_{12} & a_{22} \end{pmatrix} = \begin{pmatrix} e & & \\ & 2b + e & \sqrt{2}c \\ & \sqrt{2}c & d \end{pmatrix} \quad (4.2)$$

Δ is now block-diagonal, consisting of 1×1 and 2×2 blocks. We find that $P_1(\mu, M_s, \Delta, q)$ takes a corresponding block-diagonal form,

$$P_1(\mu, M_s, \Delta, q) = \begin{pmatrix} E(e, q) & & & & & & \\ & A_{11}(a, q) & A_{12}(a, q) & & & & \\ & A_{12}(a, q) & A_{22}(a, q) & & & & \\ & & & E(e, q) & & & \\ & & & E(e, q) & & & \\ & & & & F(f, q) & & \\ & & & & F(f, q) & & \\ & & & & & F(f, q) & \\ & & & & & F(f, q) & \end{pmatrix} \quad (4.3)$$

where

$$\begin{aligned} F(f, q) &= P_1(\mu, M_s, f, q) = \frac{fw}{w^2 - (4\mu^2 - M_s^2)\vec{q}^2 - (\mu - iq_0)^2 M_s^2} \\ &\quad (w = f^2 + \mu^2 + \vec{q}^2 + q_0^2) \\ E(e, q) &= P_1(\mu, 0, e, q) = \text{as above, with } f \rightarrow e \text{ and } M_s = 0 \\ A(a, q) &= P_1(\mu, M_s, a, q) \end{aligned} \quad (4.4)$$

Note that the function P_1 simplifies considerably when its argument is a symmetric off-diagonal 2×2 matrix, as in the e and f blocks. The resulting expressions for E and F are given on the right-hand side of (4.4). The only difficult thing in (4.4) is evaluating P_1 for the 2×2 matrix a , in which case Eqns. (A.6) and (A.7) must be used.

The only nonzero matrix elements in P_1 , on the right hand side of the gap equation, are those which are nonzero in our ansatz for Δ , on the left hand side of the gap equation. This confirms that the only color **6** terms which are induced by the color **$\bar{3}$** condensate are those which we have included in our ansatz, in agreement with the symmetry arguments given above. Although more complicated ansätze may be worth considering in future work, this ansatz is the minimal one which suffices.

Taking into account the λ and γ matrices from the gluon vertex, we end up

with the 5 gap equations

$$\begin{aligned}
e &= 4G/(2\pi)^4 \int d^4q \left(A_{11}(a, q) - \frac{5}{3}E(e, q) \right) \\
f &= 4G/(2\pi)^4 \int d^4q \left(\sqrt{2}A_{12}(a, q) - \frac{2}{3}F(f, q) \right) \\
a_{11} &= 4G/(2\pi)^4 \int d^4q \left(\frac{1}{3}A_{11}(a, q) + 3E(e, q) \right) \\
a_{12} &= 4G/(2\pi)^4 \int d^4q \left(-\frac{2}{3}A_{12}(a, q) + 2\sqrt{2}F(f, q) \right) \\
a_{22} &= 4G/(2\pi)^4 \int d^4q \frac{4}{3}A_{22}(a, q)
\end{aligned} \tag{4.5}$$

To obtain the gap parameters as a function of μ and M_s , we solve the 5 simultaneous equations (4.5) numerically, using *Mathematica*. The right-hand sides are evaluated by numerical integration of the integrands given in (4.4). For $A(a, q)$, we must evaluate $P_1(\mu, M_s, a, q)$, which corresponds to (A.7) with Δ being the 2×2 matrix a , $\kappa = 0$, and $\phi = \text{diag}(0, M_s)$. The gap parameters b, c, d, e, f determine the poles of the propagator P_1 and hence determine the quasiparticle dispersion relations and the gaps at the Fermi surface.

5 ... and Its Solutions

In this section, we present solutions to the gap equations (4.5). We demonstrate explicitly that the unlocking phase transition is first order in our model, as we have argued on general grounds in Section 2. Furthermore, we confirm that the simple criterion (2.1) is a good guide. We determine the value of M_s^{cont} , the highest strange quark constituent mass at which, in the model, no 2SC phase intrudes. We use our results to draw tentative conclusions for the behavior of strongly interacting matter as a function of density in nature.

We plot the solutions b, c, d, e, f to the gap equations along two different lines of constant M_s and one line of constant μ , all shown in Figure 3. Recall that $b = -e$ and $c = d = f = 0$ in the 2SC phase whereas all the gaps are nonzero in the CFL phase. For $M_s = 0$, $b = c$ and $e = f$. If the condensate were purely color $\bar{\mathbf{3}}$ in the CFL phase, one would have $b = -e$, $c = -f$ and $d = 0$.

Figures 4 and 5 show the solutions to the gap equations as a function of μ , for $M_s = 150$ MeV and $M_s = 350$ MeV. We see that for $M_s = 150$ MeV, the color-flavor-locked phase continues down to $\mu = 400$ MeV, below which we expect a baryonic description to become appropriate. In contrast, in Figure 5 we see that for $M_s = 350$ MeV, the CFL phase only exists for $\mu > 530$ MeV. At lower densities, below a first order unlocking phase transition, the 2SC phase is favored.⁶ This transition occurs at high enough densities that a quark matter description is

⁶In the calculations for our plots we assume M_s is the same on either side of the phase

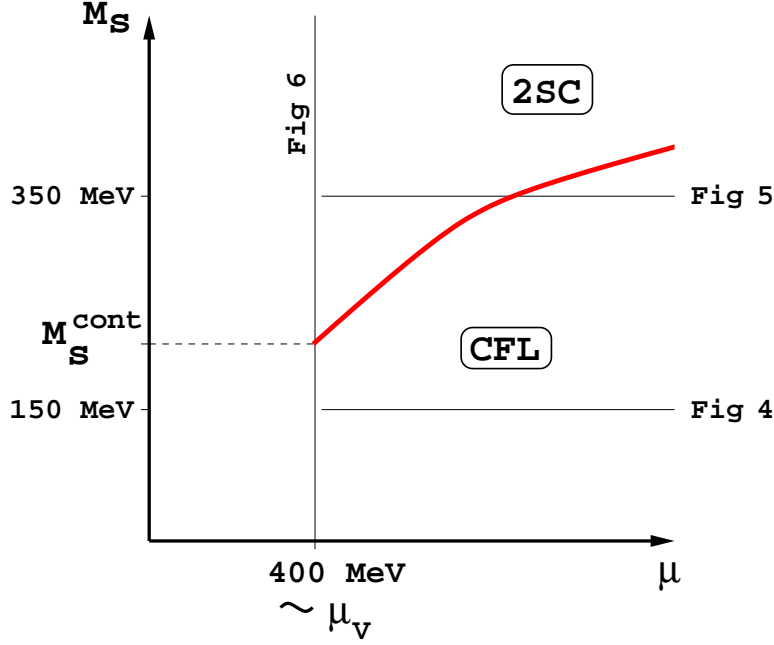


Figure 3: The part of the phase diagram in which we have done calculations using our model. The thin solid lines show the slices along which we have solved the gap equations. Note that a horizontal line in Figure 1 at some m_s corresponds to a curve in this figure which approaches the horizontal line $M_s = m_s$ from above as $\mu \rightarrow \infty$.

justified, and our model can therefore be used to describe it. At lower densities still, there is another first order phase transition to a baryonic phase.[3, 4, 5, 11, 9, 12]

In order to estimate M_s^{cont} , in Figure 6 we plot the solutions to the gap equations as a function of M_s with μ fixed at 400 MeV. This is the lowest μ at which we expect a quark matter description to be valid. We find that the CFL phase exists for M_s below a first order transition at $M_s^{\text{unlock}} = 235$ MeV. Our model therefore suggests that M_s^{cont} is of order 250 MeV.

The question, then, is whether Figure 4 or Figure 5 is closer to the behavior of strongly interacting matter as a function of density in nature. If Figure 5 shows the correct qualitative behavior, we would expect two first order phase transitions as the density is increased above nuclear density. After the first transition, one would have quark matter in the 2SC phase. In this quark matter phase, the constituent

transition. In reality M_s will be somewhat smaller in the 2SC phase because there is no chiral symmetry breaking there, but since the 2SC condensates do not involve the s quark this is of no consequence.

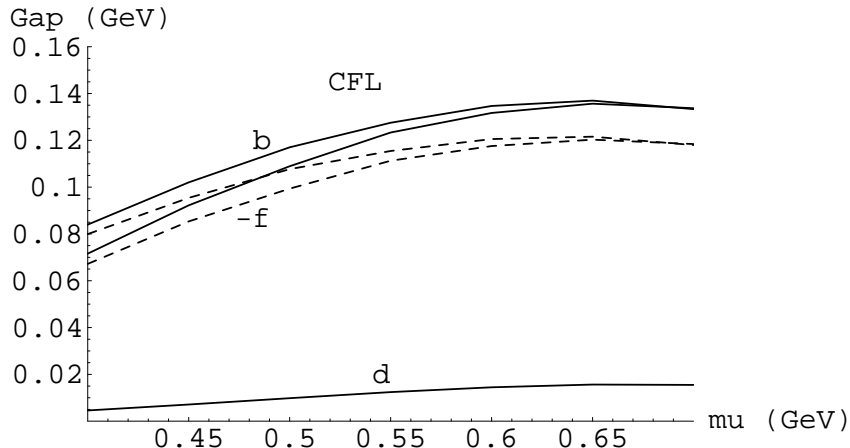


Figure 4: Solutions to the gap equations as a function of μ , at $M_s = 150$ MeV. At this value of M_s , the CFL phase persists down to $\mu = 400$ MeV, and below. The two solid lines are b and $-e$, the dashed lines are c and $-f$. At large μ , the gaps approach the $M_s = 0$ pattern.

strange quark mass must be greater than $M_s^{\text{cont}} \sim 250$ MeV. Then, above the next transition, a color-flavor-locked quark matter phase is obtained. If Figure 4 is the better guide to nature, as we surmise, then there is no window of μ in which the 2SC phase intrudes, and nature may choose a continuous transition between baryonic and quark matter with the symmetries of the CFL phase.

We have analyzed the unlocking phase transition quantitatively in our model, and can now confirm the predictions of the model-independent but qualitative arguments of Section 2. We first demonstrate that the transition is first order, and justify the location of the discontinuities shown in Figures 5 and 6. To find the first order transition in our model, we need the effective potential Ω . We use the fact that the gap equations are equivalent to the requirement that the derivative of Ω with respect to the gap parameters vanishes. The set of gap equations (4.5) corresponds to five differential equations $\partial\Omega/\partial\vec{l}|_{\text{min}} = 0$ where $\vec{l} = (b, c, d, e, f)$ at the potential minimum, so we have analytic expressions for $\partial\Omega/\partial\vec{l}$ for any value of the gap parameters \vec{l} . At a first order phase transition, Ω should have two degenerate minima, one corresponding to the CFL phase and the other to the

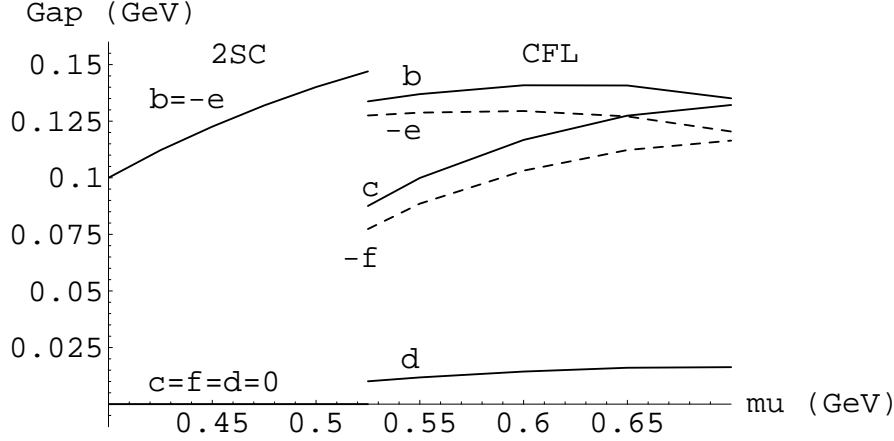


Figure 5: Solutions to the gap equations as a function of μ , at $M_s = 350$ MeV. At this large value of M_s , the CFL phase exists only for $\mu > 530$ MeV. That is, $M_s^{\text{unlock}} = 350$ MeV for $\mu = 530$ MeV.

2SC phase. We have found two minima at $M_s = 235$ MeV, $\mu = 400$ MeV. (See Figure 6.) We define a straight line $\vec{l}(x)$ in the five-dimensional space of gap parameters which goes from the 2SC minimum $\vec{l}(0) = (b = 100, c = 0, d = 0, e = -100, f = 0)$ MeV to the CFL minimum $\vec{l}(1) = (91, 56, 4, -88, -52)$ MeV. We evaluate $(\partial\Omega/\partial\vec{l})$ along this line, and then obtain the potential itself by integrating $(\partial\Omega/\partial\vec{l})(\partial\vec{l}/\partial x)$ with respect to x . The result is shown in Figure 7. The phase transition is first order.

The model-independent arguments of Section 2 lead to the criterion (2.1) for the location of the unlocking phase transition. We now compare this prediction to the quantitative results we have obtained in our model. For $\mu = 400$ MeV, at the critical strange quark mass $M_s^{\text{unlock}} = 235$ MeV (see Figure 6) the gaps c and $-f$, which vanish in the 2SC phase, are within a few MeV of each other in the CFL phase, with $c \simeq -f \simeq 55$ MeV. Taking $\Delta_{us} \simeq 55$ MeV, we find

$$(M_s^{\text{unlock}})^2 \approx 2.5\mu\Delta_{us} . \quad (5.1)$$

The unlocking phase transition in Figure 5 occurs at $M_s = 350$ MeV, $\mu = 530$ MeV

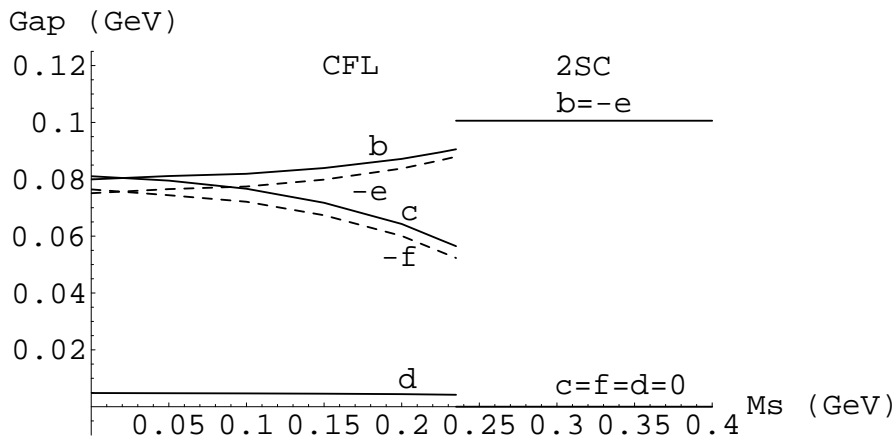


Figure 6: Solutions to the gap equations as a function of M_s , at $\mu = 400$ MeV, along the vertical line in Figure 3. When the strange quark becomes massive enough, s - u condensates become too expensive, and there is a first-order phase transition from CFL to 2SC.

and has $c \approx -f \approx 85$ MeV; this yields a relation as in (5.1), with 2.5 replaced by 2.7. We conclude that (2.1), derived by simple physical arguments based on comparing the mismatch between the up and strange Fermi momenta with the Δ_{us} gap, is a very good guide to the location of the unlocking phase transition.

6 Quark-hadron continuity

As has been emphasized in Section 4, for low enough m_s the CFL phase may consist of hadronic matter at low μ , and quark matter at high μ . This raises the exciting possibility [7] that properties of sufficiently dense hadronic matter could be found by extrapolation from the quark matter regime where models like the one considered in this paper can be used as a guide at moderate densities, and where the QCD gauge coupling becomes small at very high densities.

The most straightforward application of this idea is to relate the quark/gluon description of the spectrum to the hadron description of the spectrum in the CFL

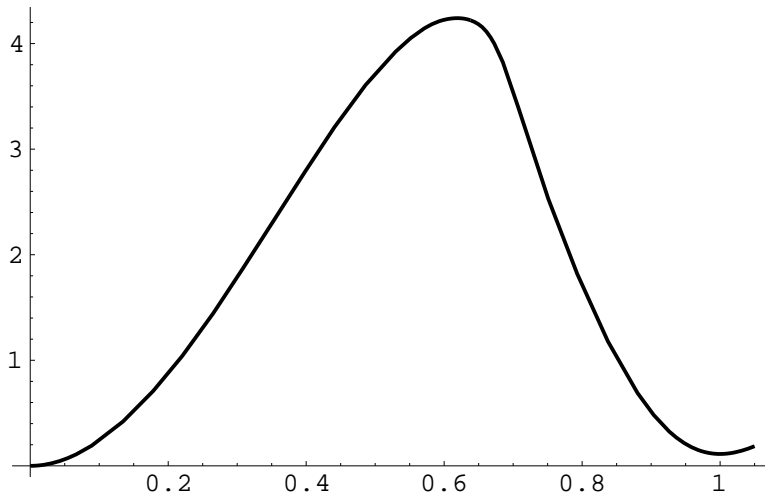


Figure 7: The effective potential Ω in units of 10^{-5} GeV^4 in the vicinity of the unlocking phase transition, for $\mu = 400 \text{ MeV}$, $M_s = 235 \text{ MeV}$. The plot corresponds to a slice of the potential in the 5 dimensional parameter space along a line which linearly interpolates between the minima in the 2SC phase ($x = 0$) and the CFL phase ($x = 1$). The phase transition is clearly first order.

phase.[7] As μ is decreased from the regime in which a quark/gluon description is convenient to one in which a baryonic description is convenient, there is no change in symmetry so there need be no transition: the spectrum of the theory may change continuously. Under this mapping, the massive gluons in the CFL phase map to the octet of vector bosons;⁷ the Goldstone bosons associated with chiral symmetry breaking in the CFL phase map to the pions; and the quarks map onto baryons. Pairing occurs at the Fermi surfaces, and we therefore expect the gap parameters in the various quark channels, calculated in Section 5, to map to the gap parameters due to baryon pairing.

In Table 2 we show how this works for the fermionic states in 2+1 flavor QCD. There are nine states in the quark matter phase. We show how they transform under the unbroken “isospin” of $SU(2)_{\text{color}+V}$ and their charges under the unbroken “rotated electromagnetism” generated by Q' , as described in Section 4. Table 2 also shows the baryon octet, and their transformation properties under the symmetries of isospin and electromagnetism that are unbroken in sufficiently dense hadronic matter. Clearly there is a correspondence between the two sets of particles.⁸ As

⁷The singlet vector boson in the hadronic phase does not correspond to a massive gluon in the CFL phase. This has been discussed in Ref. [7].

⁸The one exception is the final isosinglet. In the $\mu \rightarrow \infty$ limit, where the full 3-flavor symmetry

Quark	$SU(2)_{\text{color}+V}$	Q'	gap	Hadron	$SU(2)_V$	Q	gap
$\begin{pmatrix} bu \\ bd \end{pmatrix}$	2	+1	f	$\begin{pmatrix} p \\ n \end{pmatrix}$	2	+1	Δ_4^B
		0				0	
$\begin{pmatrix} gs \\ rs \end{pmatrix}$	2	-1		$\begin{pmatrix} \Xi^0 \\ \Xi^- \end{pmatrix}$	2	-1	
$\begin{pmatrix} ru - gd \\ gu \\ rd \end{pmatrix}$	3	0	e	$\begin{pmatrix} \Sigma^0 \\ \Sigma^+ \\ \Sigma^- \end{pmatrix}$	3	0	Δ_3^B
		+1				+1	
		-1				-1	
$ru + gd + \xi_- bs$	1	0	Δ_-	Λ	1	0	Δ_1^B
$ru + gd - \xi_+ bs$	1	0	Δ_+	—			

$$\begin{aligned}\Delta_{\pm} &= \frac{1}{2} \left(2b + e + d \pm \sqrt{(2b + e - d)^2 + 8c^2} \right) \\ \xi_{\pm} &= -\frac{1}{2c} \left(2b + e - d \mp \sqrt{(2b + e - d)^2 + 8c^2} \right)\end{aligned}$$

Table 2: Comparison of states and gap parameters in high density quark and hadronic matter.

μ increases, the spectrum described in Table 2 may evolve continuously even as the language used to describe it changes from baryons, $SU(2)_V$ and Q to quarks, $SU(2)_{\text{color}+V}$ and Q' .

If the spectrum changes continuously, then in particular so must the gaps. As discussed above, and displayed explicitly in (3.4), the quarks pair into rotationally invariant, Q' -neutral, $SU(2)_{\text{color}+V}$ singlets. The two doublets of Table 2 pair with each other, with gap parameter f . The triplet pairs with itself, with gap parameter e . Finally, the two singlets pair with themselves.

When we map the quark states onto baryonic states, we can predict that the baryonic pairing scheme that will occur is the one conjectured in Sect. 1 for sufficiently dense baryonic matter:

$$\begin{aligned}\langle p\Xi^- \rangle, \langle \Xi^- p \rangle, \langle n\Xi^0 \rangle, \langle \Xi^0 n \rangle &\rightarrow 4 \text{ quasiparticles, with gap parameter } \Delta_4^B \\ \langle \Sigma^+ \Sigma^- \rangle, \langle \Sigma^- \Sigma^+ \rangle, \langle \Sigma^0 \Sigma^0 \rangle &\rightarrow 3 \text{ quasiparticles, with gap parameter } \Delta_3^B \\ \langle \Lambda \Lambda \rangle &\rightarrow 1 \text{ quasiparticle, with gap parameter } \Delta_1^B\end{aligned}\quad (6.1)$$

is restored, it becomes an $SU(3)$ singlet, so it is not expected to map to any member of the baryon octet. We discuss this further below. The gap Δ_+ in this channel is twice as large as the others (it corresponds to Δ_1 in Ref. [6]).

The baryon pairs are rotationally-invariant, Q -neutral, $SU(2)_V$ singlets. It seems reasonable to conclude that as μ is increased the baryonic gap parameters $(\Delta_4^B, \Delta_3^B, \Delta_1^B)$ may evolve continuously to become the quark matter gap parameters (f, e, Δ_-) , which we have calculated in this paper. Assuming continuity, the magnitude of the gaps will change as the density is increased but if their ratios change less we can use our results for the gap parameters in the CFL phase at $\mu = 400$ MeV and $M_s = 150$ MeV to suggest baryonic gap parameters with ratios

$$\Delta_4^B : \Delta_3^B : \Delta_1^B \sim 1.06 : 1.26 : 1 \quad (6.2)$$

in matter which is sufficiently dense but still conveniently described as baryonic.

As mentioned above, the ninth quark corresponds to a singlet baryon which is very heavy, for reasons which have nothing to do with our considerations. We therefore expect that as μ is increased and a quark matter description takes over from a baryonic description, the density of the singlet quark/baryon becomes nonzero at some μ , and begins to increase. Deep into the quark matter phase, there is a gap Δ_+ for this ninth quark, but this does not correspond to any gap deep in the baryonic phase, because the density of the corresponding baryon is zero. There is no change in symmetry at the μ at which the density of the ninth quark/baryon becomes nonzero, just as there was no change in symmetry at the lower μ (within the “strange baryon” phase of Figure 1) at which the Ξ density became nonzero. Both these onsets are smooth transitions at arbitrarily small but nonzero temperature. We do not expect the onset of a nonzero density for the ninth quark/baryon to upset the continuity between the baryonic and quark matter phases, but symmetry arguments can only demonstrate the possibility of continuity; they cannot prove that there is no transition.

The analysis leading to (6.2) provides the first example of the use of the hypothesis of quark-hadron continuity in the color-flavor locked phase to map a quark matter calculation onto quantitative properties of baryonic matter.

7 Color-Flavor Locking at Asymptotic Densities

Son [8] has studied color superconductivity at much higher densities than those we can treat with our model, using a resummed gluon propagator rather than a point-like four-quark interaction, and has determined the leading behavior of the gap in the large μ , small $g(\mu)$ limit. Here, $g(q)$ is the QCD gauge coupling at momentum transfer q . The resulting expression,

$$\Delta \sim \mu \frac{1}{g(\mu)^5} \exp\left(-\frac{3\pi^2}{\sqrt{2}} \frac{1}{g(\mu)}\right), \quad (7.1)$$

describes the μ -dependence of the gap(s), but not their absolute normalization. Δ could be any of our gaps. The distinction between b , c , d , e and f is in the prefactor

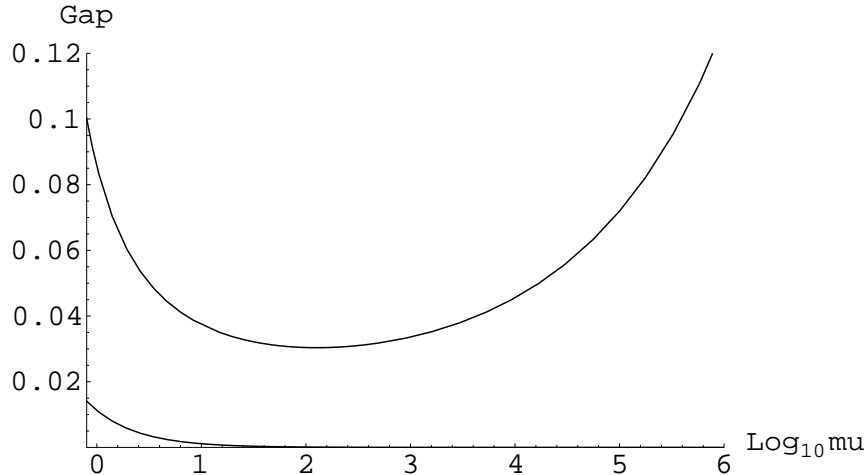


Figure 8: The upper curve shows Son’s result for the superconducting gap Δ as a function of $\log_{10} \mu$, for μ from 0.8 GeV to 10^6 GeV. The vertical scale has been normalized so that $\Delta = 0.1$ GeV at $\mu = 0.8$ GeV. We have taken $g(\mu)$ from the two-loop beta function for three flavor QCD with $\Lambda_{\text{QCD}} = 200$ MeV. Color-flavor locking occurs whenever $\Delta \gtrsim M_s^2/2\mu$. The lower curve is $M_s^2/2\mu$, taking $M_s = 150$ MeV. We conclude that QCD at very high densities is in the CFL phase.

which should appear in (7.1), but which has so far not been calculated. We take our model estimates as a guide at moderate densities, around $\mu \sim 400 - 800$ MeV, and use them to normalize the calculation of Ref. [8] by fixing the prefactor in (7.1) so that $\Delta = 100$ MeV at $\mu = 800$ MeV. We show the result in Figure 8. Note that Δ is plotted versus $\log \mu$; it changes very slowly. It decreases by about a factor of three as μ is increased to around 100 GeV (!) and then begins to rise without bound at even higher densities. We conclude that independent of any details (like the precise value of M_s , for example) at asymptotically high densities Δ is far above $M_s^2/2\mu$. For any finite value of the strange quark mass m_s , quark matter is in the color-flavor locked phase, with broken chiral symmetry, at arbitrarily high densities where the gauge coupling becomes small.

8 Conclusions

We have discussed a conjectured phase diagram for $2+1$ flavor QCD as a function of μ , the chemical potential for quark number, and m_s , the strange quark mass. We have worked at zero temperature and ignored electromagnetism and the u and d quark masses throughout. Our quantitative analysis is restricted to the high density quark matter phases, where we use a model with an effective four-fermion

interaction which has the index structure of single gluon exchange.

Our analysis shows that for any finite m_s the quarks will always pair in a color-flavor-locked (CFL) state at arbitrarily large chemical potential, breaking chiral symmetry. What happens at lower μ depends on the strange quark mass. If m_s is greater than a critical value m_s^{cont} , then as μ is reduced, there will be an unlocking phase transition to a color superconductor phase analogous to that in two flavor QCD, with restoration of chiral symmetry. We give model-independent arguments that the unlocking transition between the CFL and 2SC phases is controlled by the mismatch between the light and strange quark Fermi momenta and is therefore first order. We confirm this quantitatively in our model. If μ is reduced further, there will presumably be a phase transition to nuclear matter, and chiral symmetry will be broken again. However, if $m_s < m_s^{\text{cont}}$ then the 2SC state never occurs. The quark matter stays in the color-flavor locked phase all the way down until the transition to hadronic matter. Chiral symmetry is never restored at any μ . In this case there may be continuity between the CFL quark matter and sufficiently dense hadronic matter. Assuming such continuity, we use our calculation of quark gaps to make predictions about the gaps in hadronic matter (6.2).

At arbitrarily high densities, where the QCD gauge coupling is small, quark matter is always in the CFL phase with broken chiral symmetry. This is true independent of whether the “transition” to quark matter is continuous (as may occur for small m_s , including, we surmise, realistic m_s) or whether, as for larger m_s , there are two first order transitions, from nuclear matter to the 2SC phase, and then to the CFL phase.

There are many directions in which this work can be developed. We have worked at zero temperature, so a natural extension would be to study the effects of finite temperature. The phase diagram of two-flavor QCD as a function of baryon density, temperature and quark mass has been explored in Ref. [5]. A nonperturbative approach beyond the mean field approximation that we have employed can be performed along the lines of Ref. [20] using the exact renormalization group, or by doing a lattice calculation [21].

Within our model, one could study more exotic channels that we have ignored, such as those with $S = 1$ and/or $L = 1$, or channels that would lead to pairing of the strange quarks in the 2SC+s phase. There are also improvements that could be made to the model, such as including four- and six-fermion interactions induced by the three-flavor instanton vertex, or using sum rules to include nonperturbative gluons [22], or including perturbative gluons [8]. It would also be desirable to include the effects of electromagnetism, and of different chemical potentials for the different flavors.

Finally, it is of great importance to investigate the consequences of our findings for the phenomenology of neutron/quark stars, which are the only naturally

occurring example of cold matter at the densities we have studied. We are confident that, with the basic symmetry properties of the phase diagram now at hand, a whole new phenomenology waits to be uncovered as the role of the strange quark in dense matter is fully elucidated.

Acknowledgments

We thank E. Shuster and D. T. Son for helpful discussions. Related issues are discussed, with a different emphasis, in “Quark Description of Hadronic Phases” by T. Schäfer and F. Wilczek, IAS preprint IASSNS-HEP 99/32. We thank these authors for showing us their work prior to publication and for informative discussions. This work is supported in part by the U.S. Department of Energy (D.O.E.) under cooperative research agreement #DF-FC02-94ER40818.

Appendix A The general form of the gap equation

We calculate the gap equations for a quark-quark condensate with completely general color-flavor structure, using a four-fermion interaction vertex with the index structure of single-gluon exchange. We will allow condensation in the channels $\Delta_{ij}^{\alpha\beta} = \langle q_i^\alpha C \gamma_5 q_j^\beta \rangle$ and $\kappa_{ij}^{\alpha\beta} = \langle q_i^\alpha C \gamma_5 \gamma_4 q_j^\beta \rangle$, with arbitrary color-flavor structure. We will also allow the quark mass matrix $\phi_{ij}^{\alpha\beta}$ to have arbitrary color-flavor structure. We use the Euclidean conventions of Ref. [5]

The mean field gap equation is

$$\Sigma = -\frac{G}{(2\pi)^4} \int d^4q V_{A\mu} M^{-1}(q) V_A^\mu, \quad (\text{A.1})$$

Since we want to study quark-quark condensation, we use the Nambu-Gorkov basis, in which the quark-gluon vertex has the standard index structure

$$V_{A\mu} = \begin{pmatrix} & -\lambda_A^T \gamma_\mu^T \\ \lambda_A \gamma_\mu & \end{pmatrix}, \quad (\text{A.2})$$

and the fermion matrix M is

$$\begin{aligned} M(q) &= \begin{pmatrix} C \not{q}_+ C \\ \not{q}_- \end{pmatrix} + \Sigma, \\ \not{q}_\pm &= (q_0 \pm i\mu) \gamma^4 + q_i \gamma^i. \end{aligned} \quad (\text{A.3})$$

C is the Dirac charge conjugation matrix. In this appendix we allow Δ, κ, ϕ to have arbitrary color-flavor structure, so we treat them as general non-commuting matrices in

$$\Sigma = \begin{pmatrix} C \gamma_5 (\Delta + \kappa \gamma_4) & -i\phi \\ i\phi & (\Delta + \kappa \gamma_4) \gamma_5 C \end{pmatrix}. \quad (\text{A.4})$$

We will fix the quark masses ϕ , and solve for the superconducting gaps Δ and κ . We can just take the top left component of (A.1), which gives us

$$C\gamma_5(\Delta + \kappa\gamma_4) = \frac{G}{(2\pi)^4} \int d^4q \lambda_A^T \gamma_\mu^T X^{-1} \lambda_A \gamma^\mu, \quad (\text{A.5})$$

where $X^{-1} = (M^{-1})_{22}$, and X can be written

$$\begin{aligned} X &= \gamma_5 \left(X_1 I + X_4 \gamma^4 + X_V q_i \gamma^i + X_S q_i \sigma^{i4} \right) C \\ X_1 &= (q^2 + \mu^2)R + \phi R \phi + i(q_0 - i\mu)\Delta^{-1} \kappa R \phi - i(q_0 + i\mu)\phi \Delta^{-1} \kappa R + \Delta \\ X_4 &= i(q_0 - i\mu)R \phi - i(q_0 + i\mu)\phi R + (q_0^2 - \vec{q}^2 + \mu^2)\Delta^{-1} \kappa R + \phi \Delta^{-1} \kappa R \phi - \kappa \\ X_V &= 2q_0 \Delta^{-1} \kappa R + i(R \phi - \phi R) \\ X_S &= 2\mu R + \Delta^{-1} \kappa R \phi + \phi \Delta^{-1} \kappa R \\ R &= (\Delta - \kappa \Delta^{-1} \kappa)^{-1}. \end{aligned} \quad (\text{A.6})$$

X can now be inverted,

$$\begin{aligned} X^{-1} &= -C \left(P_1 I + P_4 \gamma^4 + P_V q_i \gamma^i + P_S q_i \sigma^{i4} \right) \gamma_5 \\ P_1 &= -(U_4^{-1} U_1 - T_4^{-1} T_1)^{-1} U_4^{-1} S_1^{-1} \\ P_4 &= -T_4^{-1} T_1 P_1 \\ U_1 &= -S_2^{-1} (-X_4 - i\vec{q}^2 X_S X_1^{-1} X_V) + S_1^{-1} (\vec{q}^2 X_V X_1^{-1} X_V - X_1) \\ U_4 &= -S_2^{-1} (-X_1 + \vec{q}^2 X_S X_1^{-1} X_V) + S_1^{-1} (i\vec{q}^2 X_V X_1^{-1} X_S - X_4) \\ T_1 &= S_2^{-1} (-X_4 - i\vec{q}^2 X_S X_1^{-1} X_V) - S_3^{-1} (-X_S + iX_4 X_1^{-1} X_V) \\ T_4 &= S_2^{-1} (-X_1 + \vec{q}^2 X_S X_1^{-1} X_S) - S_3^{-1} (iX_V - X_4 X_1^{-1} X_S) \\ S_1 &= \vec{q}^2 X_S + iq^2 X_V X_1^{-1} X_4 \\ S_2 &= \vec{q}^2 (iX_V + X_S X_1^{-1} X_4) \\ S_3 &= X_1 - X_4 X_1^{-1} X_4 \end{aligned} \quad (\text{A.7})$$

We have ignored P_V and P_S because these multiply odd powers of momentum, and so give no contribution to the integral on the RHS of the gap equation (A.5).

Note that in general $P_4 \neq 0$, so it is necessary to include κ in the ansatz. Without it the gap equations do not close. That is, if one sets κ to zero, one finds that if M_s and Δ are both nonzero, one obtains $P_4 \neq 0$ and concludes that setting $\kappa = 0$ is inconsistent. However, κ turns out to be small, and we neglect it. To check that κ is small, we solved the coupled gap equations for the κ and f gaps, in one of the 2×2 blocks of the ansatz (3.4), using a modified gluon vertex so that this block did not mix with the others. We calculated κ and f as a function of M_s , at $\mu = 400$ MeV. The values of f were very close to those obtained for the full gluon vertex (see Figure 6), and κ was zero at $M_s = 0$, and always less than 6 MeV.

References

- [1] B. Barrois, Nucl. Phys. **B129** (1977) 390. S. Frautschi, Proceedings of workshop on hadronic matter at extreme density, Erice 1978.
- [2] D. Bailin and A. Love, Phys. Rept. **107** (1984) 325, and references therein.
- [3] M. Alford, K. Rajagopal and F. Wilczek, Phys. Lett. **B422** (1998) 247.
- [4] R. Rapp, T. Schäfer, E. V. Shuryak and M. Velkovsky, Phys. Rev. Lett. **81** (1998) 53.
- [5] J. Berges, K. Rajagopal, Nucl. Phys. **B538** (1999) 215.
- [6] M. Alford, K. Rajagopal, F. Wilczek, Nucl. Phys. **B537** (1999) 443.
- [7] T. Schäfer, F. Wilczek, hep-ph/9811473.
- [8] D. Son, hep-ph/9812287.
- [9] R. Pisarski, D. Rischke, nucl-th/9811104.
- [10] M.A. Halasz, A.D. Jackson, R.E. Shrock, M.A. Stephanov, J.J.M. Verbaarschot, Phys. Rev. **D58** (1998) 096007.
- [11] J. Berges, D-U. Jungnickel and C. Wetterich, hep-ph/9811387.
- [12] G. Carter and D. Diakonov, hep-ph/9812445.
- [13] D. B. Kaplan and A. E. Nelson, Phys. Lett. **B175** (1986) 57.
- [14] T. Schäfer, F. Wilczek, hep-ph/9810509.
- [15] N. Evans, S. Hsu, M. Schwetz, hep-ph/9810514, hep-ph/9808444.
- [16] M. Iwasaki and T. Iwado, Phys. Lett. **B350** (1995) 163.
- [17] T. M. Schwarz, S. P. Klevansky and G. Papp, nucl-th/9903048.
- [18] R. Pisarski, D. Rischke, nucl-th/9903023.
- [19] T. Schäfer, private communication.
- [20] J. Berges, D-U. Jungnickel and C. Wetterich, Phys. Rev. **D 59** (1999) 034010; *ibid*, hep-ph/9811347.
- [21] S. Hands and S. Morrison, hep-lat/9902011, proceedings of “Strong and Electroweak Matter 98”, Copenhagen, Dec. 1998.

[22] N. Agasian, B. Kerbikov, V. Shevchenko, [hep-ph/9902335](#).